EBioMedicine 45 (2019) 542–552

Contents lists available at ScienceDirect

EBioMedicine

journal homepage: www.ebiomedicine.com

EBioMedicine
Published by THE LANCET

Research paper

Functional secretome analysis reveals Annexin-A1 as important paracrine factor derived from fetal mesenchymal stem cells in hepatic regeneration

Dimitra Zagoura [a,1], Ourania Trohatou [a,1], Manousos Makridakis [b], Antonia Kollia [a], Nikolitsa Kokla [a], Marika Mokou [a,b], Adriana Psaraki [a], Aristides G. Eliopoulos [a,c], Antonia Vlahou [b], Maria G. Roubelakis [a,c,*]

[a] Laboratory of Biology, School of Medicine, National and Kapodistrian University of Athens, Athens, Greece
[b] Biotechnology Laboratory, Centre of Basic Research, Biomedical Research Foundation of the Academy of Athens (BRFAA), Athens, Greece
[c] Centre of Basic Research, Biomedical Research Foundation of the Academy of Athens (BRFAA), Greece

ARTICLE INFO

Article history:
Received 30 April 2019
Received in revised form 21 June 2019
Accepted 3 July 2019
Available online 12 July 2019

Keywords:
MSCs
Secretome
Annexin-A1
Hepatic progenitors
Acute hepatic failure

ABSTRACT

Background: Human mesenchymal stem/stromal cells (MSCs) and their secreted molecules exert beneficial effects in injured tissues by promoting tissue regeneration and angiogenesis and by inhibiting inflammation and fibrosis. We have previously demonstrated that the therapeutic activity of fetal MSCs derived from amniotic fluid (AF-MSCs) and their hepatic progenitor-like cells (HPL) is mediated by paracrine effects in a mouse model of acute hepatic failure (AHF).
Methods: Herein, we have combined proteomic profiling of the AF-MSCs and HPL cell secretome with ex vivo and in vivo functional studies to identify specific soluble factors, which underpin tissue regeneration in AHF.
Findings: The anti-inflammatory molecule Annexin-A1 (ANXA1) was detected at high levels in both AF-MSC and HPL cell secretome. Further functional analyses revealed that the shRNA-mediated knock-down of ANXA1 in MSCs (shANXA1-MSCs) decreased their proliferative, clonogenic and migratory potential, as well as their ability to differentiate into HPL cells. Liver progenitors (oval cells) from AHF mice displayed reduced proliferation when cultured ex vivo in the presence of conditioned media from shANXA1-MSCs compared to control MSCs secretome. Intra-hepatic delivery of conditioned media from control MSCs but not shANXA1-MSCs reduced liver damage and circulating levels of pro-inflammatory cytokines in AHF.
Interpretation: Collectively, our study uncovers secreted Annexin-A1 as a novel effector of MSCs in liver regeneration and further underscores the potential of cell-free therapeutic strategies for liver diseases.
Fund: Fondation Santé, GILEAD Asklipeios Grant, Fellowships of Excellence – Siemens, IKY, Reinforcement of Postdoctoral Researchers, IKY.

1. Introduction

Human mesenchymal stem/stromal cells (MSCs) represent a multipotent stem cell population that is able to self-renew and differentiate into mesoderm derived cell lineages [1].Recently, MSC transplantation is emerging as a promising approach for tissue repair and its use in clinical and research applications has considerably increased [2]. Limitations of such approaches include the availability and the high number of cells for transplantation at the time needed, dosage effects, poor engraftment, a failure to understand the exact mechanisms of action, the variability in paracrine effects of the MSCs sourced from different donors and immunorejection [3,4].

Over the past decade, there has been a tremendous interest in understanding the biological and molecular mechanisms by which MSCs contribute to tissue repair and in unveiling their potential in cell therapy [2].

MSCs can modulate the inflammatory response, promote cell proliferation and repair of damaged cells and enhance tissue regeneration [5–7]. These beneficial properties make therapy based on MSCs a promising tool for tissue regeneration. Although basic research and preclinical studies have shown therapeutic effects of MSCs for tissue repair [8–10], many hurdles still exist for translating the therapeutic potential of MSCs into the clinical scale [11]. Importantly, MSCs have been the subject of clinical trials for a long time [4,12]; however the outcomes

* Corresponding author at: Developmental Biology, Laboratory of Biology, School of Medicine, National and Kapodistrian University of Athens, Michalakopoulou 176, Athens 115 27, Greece.
E-mail address: roubel@med.uoa.gr (M.G. Roubelakis).
[1] Joint first authors

https://doi.org/10.1016/j.ebiom.2019.07.009

Research in context

Evidence before this study

Current research is focused on mesenchymal stem/stromal cell (MSC)-based therapies for acute hepatic failure. The paracrine effects of MSCs have been demonstrated to play an important role in liver repair and regeneration through downregulation of proinflammatory and fibrogenic activity and stimulation of hepatocyte proliferation. However, there are limited studies regarding the MSCs secretome analysis.

Added value of this study

The present study describes, for the first time, the detailed analysis of amniotic fluid-mesenchymal stem cells (AF-MSCs) and hepatic progenitor-like (HPL) cell derived secretome. Data present the entire spectrum of paracrine factors secreted by the two cell types, and showed the important role of AF-MSC-produced ANXA1 in mediating liver repair. Importantly, our data indicated that ANXA1 represents a possible therapeutic mediator of acute hepatic failure (AHF) treatment, by its anti-inflammatory role, including effects on progenitor cell proliferation, migration and differentiation.

Implications of all the available evidence

The current study expands our understanding of the mechanisms by which MSCs confer therapeutic effects in acute hepatic failure (AHF). Moreover, it describes the first detailed analysis of AF-MSC and hepatic progenitor-like cell-derived secretome, demonstrating the important role of AF-MSC-produced ANXA1 in alleviating liver damage. Overall, these data are expected to lead to an innovative, cell free, non-invasive, less immunogenic and non-toxic alternative strategy to AHF treatment and to provide important new mechanistic information on the reparative function of progenitor cells in the liver.

have fallen short of expectations raised by encouraging in vitro and in vivo pre-clinical studies based in a wide range of disease models [4]. To this end, recent clinical trials have proven more successful in treating enterocutaneous perianal fistular disease and GvH disease in children [4].

However, due to the complex molecular mechanisms involved, crucial information on the receptors and mechanisms of action, plus their effectiveness in the context of various diseases, is often lacking. Therefore, a comprehensive and integrated validation of potential MSC therapeutics is highly warranted.

Recent work from our group and others uncovered MSC-derived conditioned media (CM) as mediators of many of the therapeutic properties of the parent cells, suggesting the development of a cell-free strategy based on MSC secretome [13–15].Various studies demonstrated that factors secreted by MSCs exhibit anti-inflammatory effects and can modulate a variety of cellular responses, such as proliferation, migration and survival [2,14,16], implying paracrine signaling as the primary mechanism of action of the therapeutic effect exerted by MSCs [17].

In our previous studies, we isolated MSCs from human second trimester AF obtained during routine amniocenteses for prenatal diagnosis [15,18–21]. We showed that these cells exhibited high proliferation rate in culture and could differentiate in vitro, not only into mesoderm derived cell types (such as adipocytes and osteoblasts), but also, into endoderm derived cells (hepatocytes) [15,18,19,21,22]. In addition, AF-MSCs represent an advantageous cell type for allogenic transplantation, by exhibiting inherently low immunogenic profile, thereby reducing the risk of cell rejection in heterologous transplantation [18–23].

We have previously shown that factors released by AF-MSCs and hepatic progenitor like (HPL) cells derived from AF-MSCs, can induce liver repair due to paracrine effects and stimulate down-regulation of the systemic inflammation by secretion of cytokines such as IL-10, in acute hepatic failure (AHF) NOD/SCID mouse model [5,24]. AHF consists a high-risk disease since the patients can develop hepatic encephalopathy and a rapid Multi-organ failure, triggering critical care management and, if unsuccessful, leading to death [25]. AHF is the culmination of severe liver cell injury from a variety of causes including viral hepatitis, adverse effects of prescription and non-prescribed drugs, toxins, metabolic disorders, and vascular insults [26,27]. Liver transplantation is the only effective therapeutic strategy, however it exhibits significant drawbacks due to organ rejection, lack of donors and high cost treatment.

In the present study, we aimed to investigate and validate, for the first time, a new concept in AHF therapy involving the study of the entire spectrum of paracrine factors secreted by AF-MSCs and HPL cells, termed as secretome, by LC-MS/MS analyses. We demonstrated high expression of Annexin-A1 (ANXA1) by HPL cells compared to AF-MSCs and confirmed the expression at protein level in cell lysates and conditioned media, by western blot analyses and ELISA. By using state-of-the-art experimental approaches for short hairpin RNA-mediated knock-down of ANXA1 and animal model-based strategies our results represent an innovative perspective in AHF therapy. In line with this, culturing liver progenitors (oval cells) derived from AHF mice with conditioned media derived from shANXA1-MSCs, resulted in the inhibition of their growth ex vivo.

Our findings provide proof-of-concept for the use of MSC secretome as an innovative, non-invasive, non-toxic and improved cell-free alternative strategy for liver repair and provide the impetus to validate the broader therapeutic applications of MSC secretome in other tissue-destructive diseases.

2. Material and methods

2.1. Isolation and culture of AF-MSCs

The AF-MSCs were isolated and cultured according to the methods described in previous studies [18,19]. All samples were collected following written informed consent, approved by the Ethical Committee of Alexandra Hospital, Athens, Greece, the Bioethics Committee of the School of Medicine of the University of Athens and the Bioethics Committee of the Biomedical Research Foundation of the Academy of Athens (BRFAA). Spindle-shaped colonies, termed as AF-MSCs, were used in the present study, derived from 6 human AF samples. Colonies of freshly isolated cells (passage 0) were selected and cells were subcultured. Cells, at passage 10–22 and at 80% confluency, were used for hepatogenic differentiation. AF-MSCs at passage 22–30 were used for proteomic analysis.

2.2. Hepatogenic differentiation of AF-MSCs

To induce hepatogenic differentiation, AF-MSCs (passage 10–22) or AF-MSCs transduced with shANXA1 or shscramble (passage 10–22), from 6 different AF samples, were cultured in serum-deprived media for 2 days [Iscove's modified Dulbecco medium (IMDM, Thermo Fisher Scientific Inc., Waltham, MA USA) containing 20 ng/ml epidermal growth factor (EGF, Peprotech, London, UK) and 10 ng/ml basic fibroblast growth factor (bFGF, Peprotech)]. Then, cells were treated with initiation medium, containing IMDM supplemented with 20 ng/ml hepatocyte growth factor (HGF, Peprotech), 10 ng/ml bFGF and 0.1% dimethyl sulfoxide (DMSO, Sigma-Aldrich Ltd., St. Louis, MO USA) for 7 days. These cells were termed hepatic progenitor-like cells (HPL

cells). To further differentiate HPL cells into hepatocyte-like cells (HL cells), HPL cells were treated with maturation medium consisting of IMDM supplemented with 20 ng/ml oncostatin M (Peprotech), 1 μM dexamethasone (Sigma-Aldrich Ltd.) and ITS (Sigma-Aldrich Ltd.) for 2 weeks, as previously described [15,19] passage 10–22.

To determine hepatogenic differentiation, glycogen production was assessed by Periodic Acid-Schiff (PAS) stain (Sigma-Aldrich Ltd.) according to the manufacturer's protocol. Photographs (20×) were taken using an inverted microscope Leica BMIRE2 and software LAS v3.8. Finally, PAS staining was quantified using Image J v1.43m software.

2.3. Real-time quantitative PCR

A detailed protocol for Real-time quantitative PCR analysis is provided in Supplementary material and methods.

2.4. Conditioned media (CM) collection for proteomic analysis

One and a half million AF-MSCs and HPL cells were cultured in their specific media, as it is described in the previous section. At 80% confluency the media were removed and the cell layers were washed 3 times with 1xPBS (Gibco BRL, Grand Island, NY) and 1 time with serum and phenol red free medium (SFM) (Gibco-Invitrogen, Grand Island, New York). Cells were then incubated with SFM for 24 h and then conditioned media (CM) were collected as previously described [28]. The latter was centrifuged at 1000 ×*g* for 10 min at 4 °C to remove dead cells and large debris and incubated with 7.5% Trichloro Acetic Acid (TCA) (Fluka, Buchs Switzerland), 0.1% NLauroyl Sarcosine (NLS) (Fluka) at −20 °C overnight. Centrifugation then followed at 10,000 ×*g* for 10 min at 4 °C. The supernatant was discarded, and the pellet was washed in ice cold Tetra Hydro Furan (THF) (Sigma-Aldrich Ltd.) and centrifuged again as previously. The final pellet was air dried and resuspended in sample buffer [7 M urea (Applichem, Darmstadt, Germany), 2 M thiourea (Fluka), 4% CHAPS (Applichem), 1% DTE(Sigma), 2% IPG buffer (BioRad) and 3.6% Protease inhibitors (BioRad)] followed by 30 min bath sonication. Samples were stored at −80 °C until use.

2.5. Sample preparation for proteomic analysis

Samples were prepared using the GeLC-MS method as previously described [29]. Briefly, ten micrograms of each sample were analyzed in SDS-PAGE. Electrophoresis was terminated when samples just entered the separating gel. Gels were stained with coomassie colloidal blue overnight. Each band was excised from the gel and further sliced to small pieces (1-2 mm). Gel pieces were destained with 40% Acetonitrile (Sigma), 50 mM NH_4HCO_3 (Fluka), reduced with 10 mM DTE (Sigma) in 100 mM NH_4HCO_3 for 20 min RT and alkylated with 54 mM Iodoacetamide (Applichem) in 100 mM NH_4HCO_3 for 20 min RT in the dark. Samples were then washed with 100 mM NH_4HCO_3 for 20 min at RT, followed by another wash with 40% Acetonitrile, 50 mM NH_4HCO_3 for 20 min at RT and a final wash with ultrapure water under the same conditions was performed. Gel pieces were dried in a centrifugal vacuum concentrator and trypsinized overnight in the dark, RT, by adding 600 ng of trypsin (Roche) per sample (trypsin stock solution: 10 ng/μl in 10 mM NH_4HCO_3, pH 8.5). Peptides were extracted after incubation with the following buffers: 50 mM NH_4HCO_3 for 15 min, RT followed by two incubations with 10% Formic Acid, Acetonitrile (1:1) for 15 min, RT. Peptides were eluted in a final volume of 600 μl and filtered with PVDF filers (Merck Millipore) before dried in a centrifugal vacuum concentrator. Dried peptides were reconstituted in mobile phase A buffer (0.1% formic acid, pH 3) and processed with LC-MS/MS analysis.

2.6. LC-MS/MS

LC-MS/MS experiments were performed on the Dionex Ultimate 3000 UHPLC (Thermo Fisher Scientific, Bremen, Germany) system coupled with the high-resolution nano-ESIOrbitrap-Elite mass spectrometer (Thermo Fisher Scientific). Each sample was reconstituted in 10 μl loading solution consisted of 0.1% *v*/v formic acid. A 5 μl volume was injected and loaded on the Acclaim PepMap 100 (100 μm × 2 cm C18, 5 μm, 100 Å) trapping column with the ul-Pick-Up Injection mode with the loading pump operating at a flow rate of 5 μl/min. For the peptide separation the Acclaim PepMapRSLC, 75 μm × 50 cm, nanoViper, C18, 2 μm, 100 Å column (Thermo Fisher Scientific) retrofitted to a PicoTip (New Objective Woburn, MA, USA) emitter was used for multi-step gradient elution. Mobile phase (A) was composed of 0.1% formic acid and mobile phase (B) was composed of 100% acetonitrile, 0.1% formic acid. The peptides were eluted under a 240 min gradient from 2% (B) to 33% (B). Flow rate was 300 nl/min and column temperature was set at 35 °C. Gaseous phase transition of the separated peptides was achieved with positive ion electrospray ionization applying a voltage of 2.5 kV. For every MS survey scan, the top 10 most abundant multiply charged precursor ions between *m*/*z* ratio 300 and 2200 and intensity threshold 500 counts were selected with FT mass resolution of 60,000 and subjected to HCD fragmentation. Tandem mass spectra were acquired with FT resolution of 15,000. Normalized collision energy was set to 33 and already targeted precursors were dynamically excluded for further isolation and activation for 30 s with 5 ppm mass tolerance.

2.7. MS data processing

MS data processing methodology is provided in Supplementary material and methods.

2.8. In silico analyses

The in silico analysis is provided in Supplementary material and methods section.

2.9. Lentiviral vector construction and transduction of AF-MSCs

The knockdown studies were performed using lentiviral-mediated RNA interference. The lentiviral vectors with the sequences for the shRNAs were purchased from the Erasmus Center for Biomics (https://www.erasmusmc.nl/cs-research/erasmusmcresearch/biomics?lang=en). A scrambled shRNA (shscramble) was used as control, as previously described [30]. The shRNA sequence used to knockdown the expression levels of ANXA1 was the following:CCGGGCCTTGTATGAAGCAGGAGA ACTCGAGTTCTCCTGCTTCATACAAGGCTTTTTG. For the lentivirus production, a four plasmid system was used for the transient transfection of 293 T cells as previously described [30], followed by concentration with Amicon Ultra Centrifugal Filters-100 K Units (Merck KGaA, MA, USA). The titers of the concentrated lentiviruses were determined after infection of AF-MSCs cells with serial dilutions of the viral stock. The lentiviral titers were estimated at 10 [5]–5 × 10^5 infectious units (IU)/ml. For transduction, 5 × 10^4 AF-MSCs per well were seeded into 12-well plates and lentivirus was added at a multiplicity of infection (MOI) of 5 (AF-MSC-shANXA1).As a control, AF-MSCs transduced with a lentivirus for shscramble was used at the same MOI (AF-MSC-shscramble). After seven days, selection with 0.5 μg/ml puromycin (Sigma-Aldrich Ltd.) was performed for five days.

2.10. Western blot analysis

A detailed protocol is provided in Supplementary material and methods.

2.11. Colony-forming unit assay

The clonogenic potential of AF-MSCs after knockdown expression of ANXA1 was estimated by performing a colony forming unit (CFU-F)

assay. Specifically, transduced AF-MSCs with shANXA1 or shscramble lentiviruses were plated at three clonal densities (70, 140 and 280 cells) per 60-mm plates for 14 days at 37 °C in a humidified, 5% CO_2 incubator and then stained with Crystal Violet (Sigma-Aldrich Ltd.). Photographs were taken from 5 fields of view (×10 or ×5) for each well, using a Leica CTR MIC microscope. The number of CFU-Fs was estimated per 100 MSCs initially plated, based on a linear regression analysis of the three different initial cell concentrations as previously described [22,31]. The data are presented as the mean ± SDV of three independent experiments (3 samples per experiment, n = 3).

2.12. MTS proliferation assay

A detailed protocol is provided in Supplementary material and methods.

2.13. Apoptosis assay

AF-MSCs transduced with shANXA1 or shscramble lentivirus were assessed by Annexin V–FITC staining (Biolegend Inc., CA, USA), according to the manufacturer's instructions. For live-dead cell discrimination, 7AAD (Sigma-Aldrich Ltd.) staining was used. Flow cytometry was performed using the Beckman Coulter Cytomics FC 500 flow cytometer (Beckman Coulter Ltd., Palo Alto, CA, USA).

2.14. Transwell migration assay

To study the effect of ANXA1 in the migration properties of AF-MSCs, in vitro migration assay was performed, as described in our previous studies [32]. In more detail, 1.5×10^4 AF-MSCs, AF-MSC-shscramble or AF-MSC-shANXA1 cells, were transferred to the insert of transwell plate with pore size of 8 μm (Sigma-Aldrich Ltd.) in 100 ml DMEM supplemented with 0.5% FBS. The cells were allowed to migrate for 16 h, towards coated wells with 10 μg/ml fibronectin (Sigma-Aldrich Ltd.) and supplemented with DMEM (0.5% FBS). Migrated cells were fixed with 4% paraformaldehyde (Sigma-Aldrich Ltd) on the underside of the membrane and then stained with hematoxylin and eosin (Sigma-Aldrich Ltd.). Photographs of nuclei were taken (20×) for each membrane using an inverted microscope Leica BMIRE2 and software LAS v3.8. Three independent experiments (3 samples per experiment, n = 3) were performed and the mean ± SDV of each experiment was calculated.

2.15. Measurement of ANXA1 release

AF-MSCs, AF-MSC-shscramble and AF-MSC-shANXA1 cells (passage 5–13) were cultured until 80% confluency. Three samples of 1.5×10^6 AF-MSC-shscramble and AF-MSC-shANXA1 cells (n = 3) were further treated with serum-free DMEM culture medium without phenol red for 24 h. CM were collected, centrifuged at 1000rcf for 5 min and concentrated 25-fold using ultrafiltration units with a 3 kDa cutoff prior used for ELISA (Millipore, Bedford, MA, USA). Released ANXA1 in CM was measured by using a commercially available ELISA kit (Wuhan Fine Biotech Co., Ltd., China). The absorbance was determined by a microplate reader at 450 nm (ELX 800, Biotek Instruments Inc., VT, USA). Three independent experiments were performed and the mean ± SDV of each experiment was calculated.

2.16. Cytokine analysis

Quantification of blood serum levels of mouse interleukins, derived from 5 mice (n = 5) was performed by using commercially available ELISA kits for IFN-γ (Becton Dickinson, San Jose, CA) and TNF (Bender MedSystems GmbH, Vienna, Austria). Three independent experiments were performed and the mean ± SDV of each experiment was calculated.

2.17. CM preparation for in vitro and in vivo studies

For the preparation of the CM, $1,5 \times 10^6$ AF-MSCs, AF-MSC-shscramble and AF-MSC-shANXA1 cells (passage 5–13) were cultured until 80% confluency. Further, the cells were allowed to grow for 48 h in DMEM containing 0.5% FBS to prevent protein aggregation. CM were collected, centrifuged at 1000 rcf for 5 min to remove cell debris and further concentrated 25-fold using ultrafiltration units with a 3 kDa cutoff prior to ELISA testing (Millipore, Bedford, MA, USA).

2.18. Oval cells isolation

A detailed protocol is provided in Supplementary material and methods.

2.19. Oval cells proliferation assay

Oval cells were seeded in a 96 well plate at a density of 1.5×10^4/well in 5 replicates and incubated with CM derived from AF-MSCs, AF-MSC-shscramble and AF-MSC-shANXA1 cells. DMEM (20% FBS) and DMEM (0.5% FBS) were also used as positive and negative control, respectively. MTS assay (Promega Ltd) was performed after 3 days in culture and the absorbance was measured at 492 nm and at 595 nm as reference wavelength by the ELISA plate reader (Multiskan GO version 1.01.10, Thermo Scientific). The proliferation rate of oval cells was estimated using the following formula: $[(OD_{day\ x} - OD_{day\ 0})/(OD_{day\ 0})$ x100]. The experiment was performed in triplicates and the mean of each experiment was calculated.

2.20. Mouse models and conditioned media (CM) administration protocol

NOD/SCID mice were housed and maintained at the Animal Facility of the BRFAA. The procedures for the care and treatment of animals were performed according to the Institutional guidelines, which follow the guidelines of the Association for Assessment and Accreditation of Laboratory Animal Care, the recommendations of the Federation of European Laboratory Animal Science Associations and of the National Institute of Health. For the induction of acute hepatic failure (AHF), NOD/SCID mice (n = 5) aged 6 to 8 weeks were administered intraperitoneally with a single dose of 0,5 ml/kg body weight CCl_4 dissolved in sun oil, whereas control animals (n = 5) received phosphate buffered saline only. The following day, mice (n = 5 per group) underwent intrahepatic administration of CM derived from AF-MSCs, AF-MSC-shscramble and AF-MSC-shANXA1 cells as described before [3]. The administration procedure included the insertion of a 29-gauge spinal needle in the left liver lobe which was initially detected by ultrasound imaging [Ultrasound Vivid7, 13iL (14-MHz/GE) linear array echo transducer, Georgia, USA], after hair removal, as described in our previous studies [15].

2.21. Assessment of liver functions

Twenty-four hours after CM administration, the mice (n = 5 per group) were sacrificed and blood samples were collected and centrifuged at 11,000 rcf for 5 min, to allow blood coagulation. The serum from each mouse was collected separately and measured for the levels of aminotransferase (AST) and alanine aminotransaminase (ALT) in an automatic biochemical analyzer (Medilyzer-Medicon Hellas).

2.22. Histochemical analyses of mice liver sections after CM administration

These assays relied on well-established procedures and are provided in Supplementary material and methods.

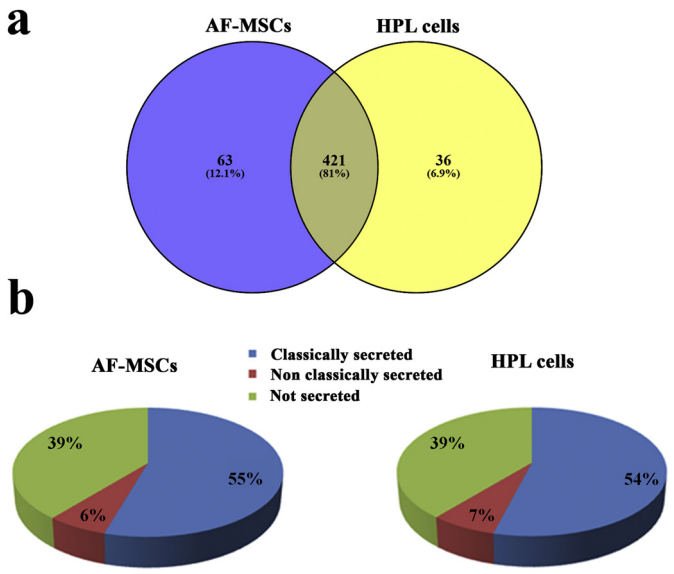

Fig. 1. Analysis and classification of the identified proteins in AF-MSCs and HPL cells. (a) Venn diagrams showing the high percentage of overlapping proteins among the secretome of the two groups (AF-MSCs vs HPL). The information shown in the Venn diagram has been derived after the frequency threshold application (only peptides identified in 3/4 samples in at least one group were considered for further analysis) in the total number of identifications obtained in the two groups of samples. (b) Classification of the identified proteins. The high percentage (61%) of secreted proteins (classically and non-classically secreted) obtained in both groups, indicates the efficiency of the utilized protocol for the enrichment of secreted proteins.

2.23. Ingenuity pathway analysis (IPA)

The bioinformatics analysis based on IPA is provided in Supplementary material and methods.

2.24. Statistical analysis

The Student's *t*-test method was used to determine the statistical significance, and p values are indicated in the figures, where * represents $p < 0.05$, ** represent $p < 0.01$ and *** represent $p < 0.001$. Mean values and confidence level are reported in Supplementary Table S3. MS data analysis was performed as previously described [33]. Peptides identified in 75% of the samples (3/4 replicates) in at least one group were further processed for quantification and statistical analysis. Mann-Whitney test was applied for the statistical analysis. Statistically significant proteins ($p \leq 0.05$) with a fold change of ≥1.5 were considered as differentially expressed (Supplementary Table S2).

3. Results

3.1. Characterization and comparison of AF-MSC and HPL secretome profiles by LC-MS/MS

The secretome of AF-MSCs and HPL cells was analyzed by high resolution LC-MS/MS analysis. Four biological replicates per group were included in the analysis. A mean value of 737 ± 80 protein identifications was obtained from the AF-MSC secretome, whereas in the HPL secretome the mean value of identified proteins was 679 ± 32 (Supplementary Table S1). Quantification was performed at the peptide level: peptides identified in 75% of the samples (3/4 replicates) in at least one group were further processed for quantification and statistical analysis. After applying the aforementioned frequency threshold in the dataset, 484 proteins were selected in the AF-MSC secretome and 457 proteins in the HPL secretome, respectively (Fig. 1a, Supplementary Table S2). The overlapping identifications among the two groups were 421 (81%), whereas 63 proteins (12.1%) were only identified in the AF-MSC secretome and 36 proteins (6.9%) in the HPL secretome (Fig. 1a & Supplementary Table S2). Of note, the majority of the proteins

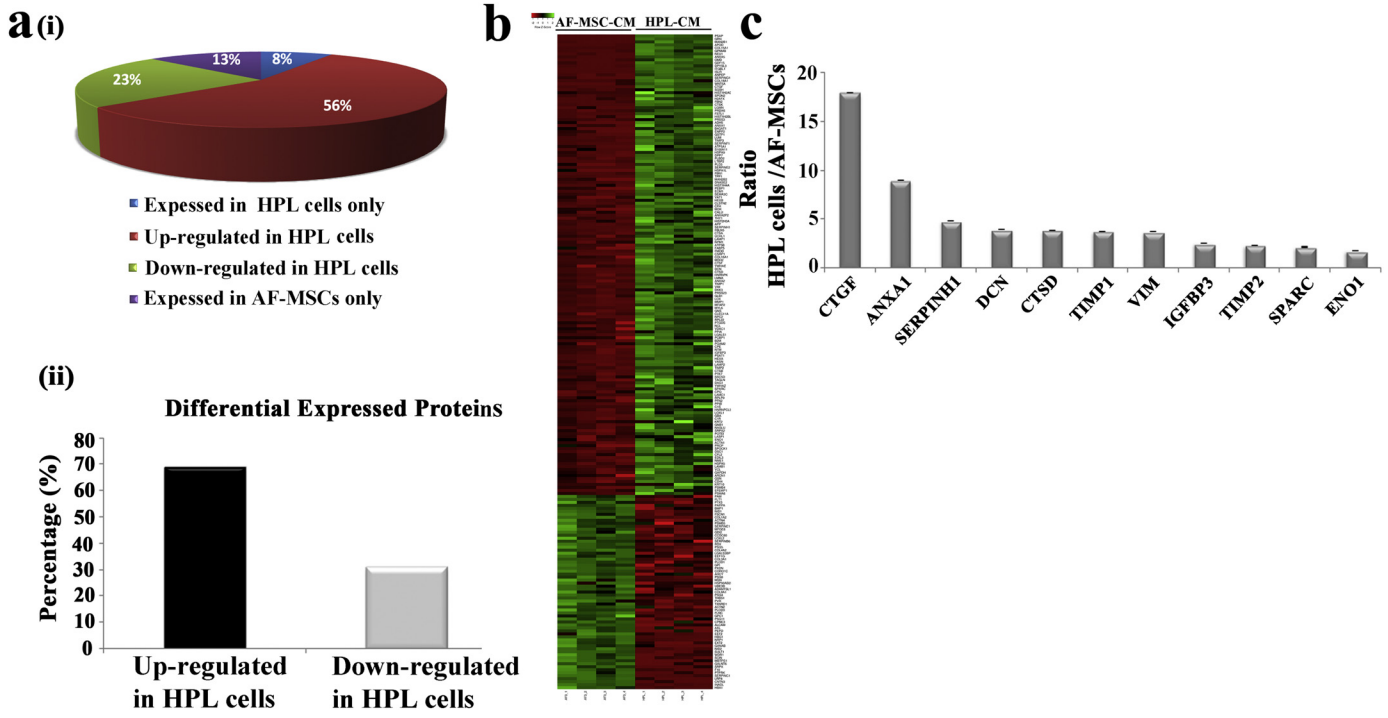

Fig. 2. Comparative proteomic analysis between the HPL and AF-MSC secretome. (a) (i) Pie chart illustrates the percentage of the proteins that were common and differentially expressed (fold change<0.67 or > 1.5, $p < 0.05$) between HPL cells and AF-MSCs, as well as of the proteins that were uniquely expressed per category. (ii) Bar graph representing the percentage of the 219 differentially expressed proteins that were statistically significant upregulated or downregulated in the secretome of HPL cells versus AF-MSCs. (b) The heat map illustrates the expression level changes of the 219 differentially expressed proteins among the HPL and the AF-MSC CM samples. Green color indicates up-regulation whereas red color indicates down regulation of the reported proteins. (c) Bar graph representing the relative expression levels of selected secreted proteins in HPL cells vs AF-MSCs.

was predicted to be secreted by signal peptide triggered secretion (55% for AF-MSCs, 54% for HPL) and non-classical secretion (6% for AF-MSCs, 7% for HPL) (Fig. 1b). The high percentage of secreted proteins (61% for each group) verifies the efficiency of the applied protocol for conditioned media (CM) collection [28,34]. After performing quantification and statistical analysis, 154 proteins (56%) were found at higher levels in the HPL secretome compared to the AF-MSCs CM (HPL/AF-MSC ratio: >1.5; Mann Whitney test, $p < 0.05$), whereas 65 proteins (23%) were found reduced in the HPL CM compared to the AF-MSC CM (HPL/AF-MSC ratio: <0.67; Mann Whitney test, $p < 0.05$). Thirty-five proteins (13%) detected only in the AF-MSC CM and 22 proteins (8%) only in HPL CM reached statistical significance (Supplementary Table S2 & Fig. 2a i, ii). The differentially expressed proteins between the HPL and AF-MSC CM are presented in Fig. 2b.

3.2. Annexin-A1 is increased in conditioned medium (CM) from HPL compared to AF-MSC cultures

In our previous publication [15] we have shown that HPL CM was found to be more efficient than CM derived from AF-MSCs in treatment of the damaged liver. For this reason we selected proteins found at higher levels in HPLCM compared to AF-MSCCM (Fig. 2c) for further examination. Among them, we observed a significant number of fibrosis-related molecules in HPLCM, including Vimentin (VIM), an intermediate filament protein with wound healing and liver regeneration ability [12,35], cathepsin D (CTSD), metalloproteinase inhibitor 1 and 2 (TIMP1, TIMP2), connective tissue growth factor (CTGF), SPARC, SERPINH1 and anti-fibrotic molecules Decorin (DCN) and Insulin-like growth factor-binding protein 3 (IGFBP3). However, we were particularly intrigued by the elevated levels of Annexin-A1 (ANXA1) in HPL compared to AF-MSC CM (HPL/AF-MSC ratio: 8.97, $p < 0.05$) because of its reported anti-fibrotic and anti-inflammatory properties [36–38].

To enable further analyses of the role of secreted ANXA1 in liver regeneration, we established a lentivirus-mediated RNA interference (shRNA) system to knock-down ANXA1. Thus, AF-MSCs (passage 10–22) were transduced with lentivirus expressing a shANXA1 sequence (AF-MSC-shANXA1) or a scramble control (AF-MSC-shscramble) and cellular ANXA1 levels were assessed by Western blot. We observed a statistically significant decrease in ANXA1 expression in AF-MSC-shANXA1 compared with AF-MSCs (0.57 ± 0.13 fold expression difference, $p < 0.01$, Student's *t*-test) (Fig. 3a). In contrast, AF-MSC-shscramble and AF-MSCs exhibited similar ANXA1 expression levels (0.94 ± 0.12 fold expression difference) (Fig. 3a).

We next determined the levels of ANXA1 released in the conditioned media, by using ELISA and Western blot analyses. The evaluation of ANXA1 immunoreactivity in CM samples by ELISA revealed a 79.4% reduction in ANXA1 secreted by AF-MSC-shANXA1 compared to AF-MSC-shscramble cells ($p < 0.0001$, Student's *t*-test) (Fig. 3B). Immunoblot analysis of CM from AF-MSC-shANXA1 versus AF-MSC-shscramble cultures confirmed the ELISA results (0.2 ± 0.03 fold

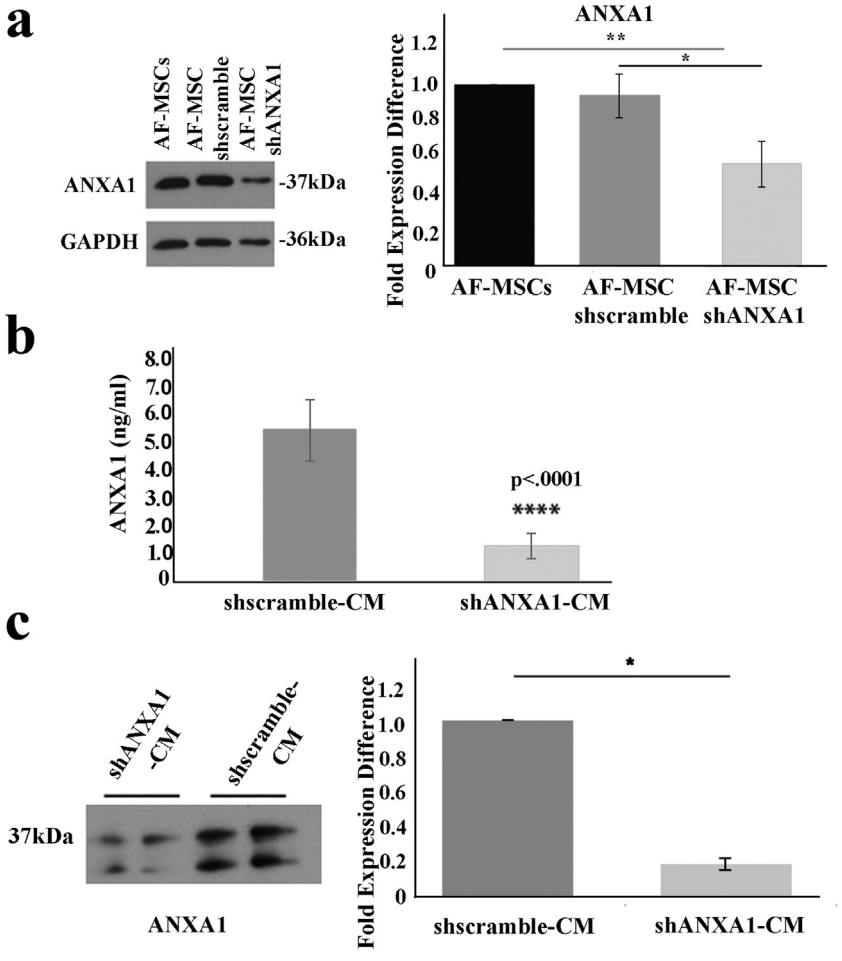

Fig. 3. Lentiviral mediated RNAi knockdown of ANXA1 reduces the molecule's expression in AF-MSCs and their secretome. (a) Western blot analysis of ANXA1 in AF-MSCs, AF-MSC shscramble and AF-MSC shANXA1. Quantification was performed using the Quantity One software and the results were normalized to GAPDH positive control and then to AF-MSCs. (b) ELISA analysis of ANXA1 expression levels in shscramble-CM and shANXA1-CM. Data presented as mean ± SD of at least three independent experiments and analyzed by Student's test (****$p < 0.0001$). (c) Western blot analyses of the secreted ANXA1 in conditioned media (CM) derived from AF-MSC-shANXA1 and AF-MSC-shscramble. The densitometry analysis of the results was performed using the Quantity One software. Data presented as mean ± SD of two independent experiments and analyzed by Student's test (*$p < 0.05$).

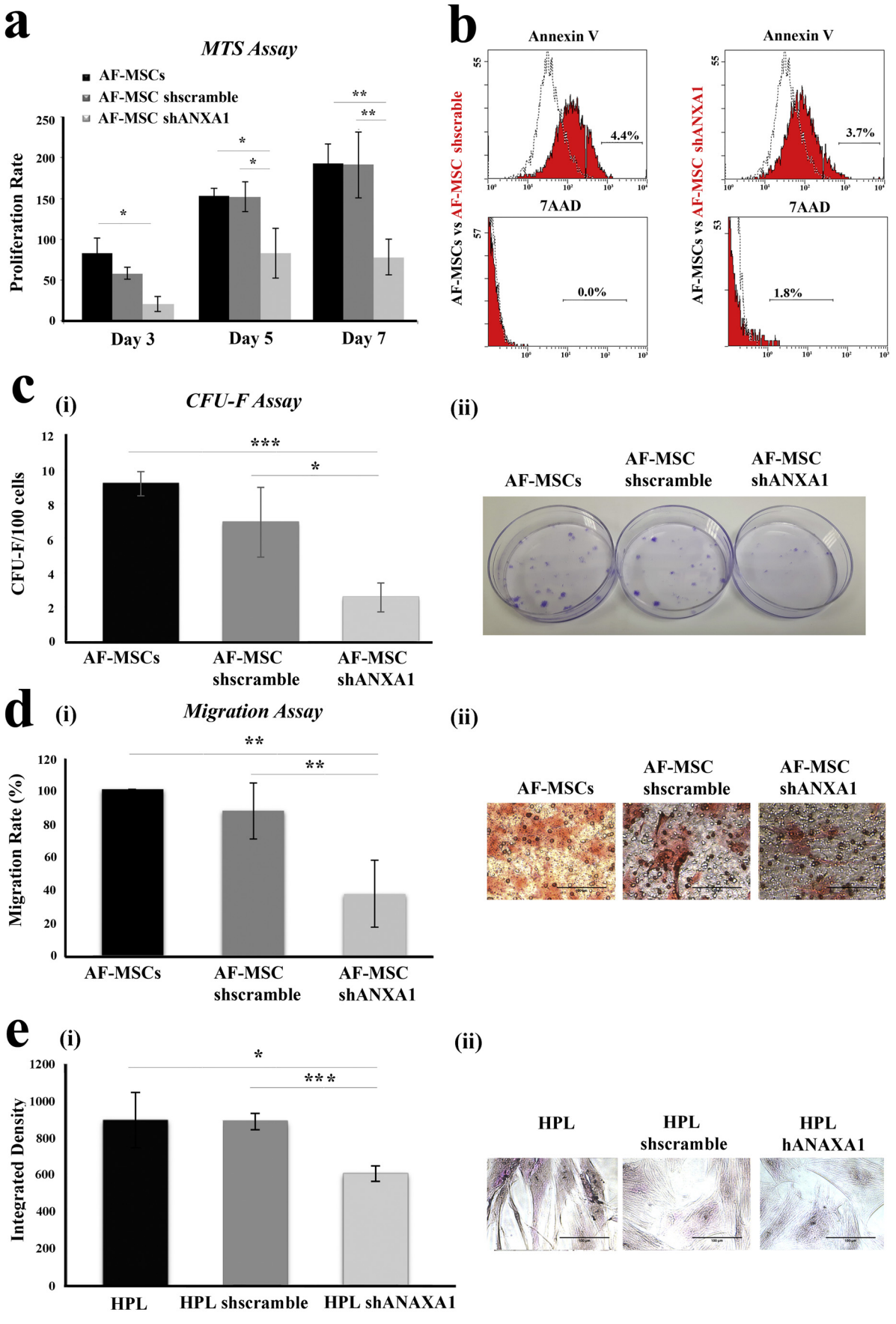
a
MTS Assay
AF-MSCs
AF-MSC shscramble
AF-MSC shANXA1
Proliferation Rate
Day 3
Day 5
Day 7
b
Annexin V
Annexin V
AF-MSCs vs AF-MSC shscrable
AF-MSCs vs AF-MSC shANXA1
4.4%
3.7%
7AAD
7AAD
0.0%
1.8%
c
(i)
CFU-F Assay
CFU-F/100 cells
AF-MSCs
AF-MSC shscramble
AF-MSC shANXA1
(ii)
AF-MSCs
AF-MSC shscramble
AF-MSC shANXA1
d
(i)
Migration Assay
Migration Rate (%)
AF-MSCs
AF-MSC shscramble
AF-MSC shANXA1
(ii)
AF-MSCs
AF-MSC shscramble
AF-MSC shANXA1
e
(i)
Integrated Density
HPL
HPL shscramble
HPL shANAXA1
(ii)
HPL
HPL shscramble
HPL hANAXA1

expression difference, $p < 0.05$, Student's *t*-test) (Fig. 3c). These findings validate ANXA1 as a component of the AF-MSC secretome.

3.3. The knock-down of ANXA1 alters the functional properties of MSCs

The aforementioned observations prompted us to initially explore the impact of ANXA1 on major functional properties of AF-MSCs. To this end, we examined the effects of ANXA1 knock-down on AF-MSC proliferation, migration, clonogenicity and capacity to differentiate into HPL cells.

Cell growth was assessed by using MTS assays at different time intervals (3, 5 and 7 days). As shown in Fig. 4a, the knock-down of ANXA1 in AF-MSCs resulted in a significant reduction in cell growth compared with AF-MSC-shscramble and AF-MSCs (day 7: 40.82% and 41.27% respectively). As the MTS assay cannot dissociate between reduced proliferation and elevated cell death, we analyzed AF-MSC-shANXA1 and control cultures for apoptosis using flow cytometry of Annexin V and 7AAD stained cells. The results showed that neither early apoptosis (Annexin V^+) nor late apoptosis/necrosis ($7AAD^+$) was affected by the knock-down of ANXA1 in MSCs (Fig. 4b). Subsequent experiments were performed to determine the clonogenic potential of these cells. AF-MSC-shANXA1 showed a statistically significant reduction in clonogenic potential (2.6 ± 0.83 CFU-F/100 cells, $p < 0.001$, Student's *t*-test) compared with AF-MSCs (9.2 ± 0.72 CFU-F/100 cells) (Fig. 4c i, ii). Furthermore, we evaluated the migratory capacity of AF-MSC-shANXA1 compared with AF-MSC-shscramble and AF-MSCs using transwell assays. AF-MSC-shANXA1 were found to exhibit 62.84% ($p < 0.01$, Student's *t*-test) migratory impairment compared to AF-MSCs, whereas AF-MSC-shscramble exhibited similar migratory potential with AF-MSCs (Fig. 4d i, ii). Finally, as AF-MSCs are able to give rise to HPL cells (Supplementary Fig. S1) [15,19], we evaluated the impact of ANXA1 knock-down on the differentiation potential of AF-MSCs by assessing the glycogen storage capacity of HPL. The results showed that HPL-shANXA1 exhibited a significant decrease in glycogen storage which is 32.66% and 31.65% compared with HPL and HPL-shscramble respectively ($p < 0.001$, $p < 0.05$, Student's *t*-test), (Fig. 4e i, ii). We conclude that the knock-down of ANXA1 impairs AF-MSC proliferation, migration, clonogenicity and capacity to differentiate into HPL cells.

3.4. Secreted ANXA1 confers anti-inflammatory effects in a mouse model of AHF

Given the established therapeutic effect of AF-MSCs in acute liver injury [15], we hypothesized that ANXA1 secreted by AF-MSCs may be a component of this response. To address this hypothesis, NOD/SCID mice were intraperitoneally injected with CCl_4 which induces hepatocellular apoptosis, periportal necrosis and inflammatory cell infiltration, as confirmed by H&E staining of liver sections (Fig. 5a). Twenty-four hours later, CM from AF-MSC-shscramble or shANXA1 cultures was administered into the left liver lobe of CCl_4-treated mice and liver damage was monitored by histology (H&E staining) and assessment of serum levels of ALT/AST transaminases. It was found that administration of CM from AF-MSC-shscramble cultures reduced the histological manifestations of tissue damage (Fig. 5a) and lowered AST (SGOT) and ALT (SGPT) levels by 82.76% and 90% respectively compared to control CCl_4-treated mice ($p < 0.05$, $p < 0.01$, Student's *t*-test) (Fig. 5b). In contrast, intrahepatic injection of CM from shANXA1 cultures failed to exert a significant effect on serum AST and ALT levels (Fig. 5b), and was accompanied by extensive hepatocellular apoptosis and inflammatory cell infiltration (Fig. 5a). ANXA1, among other secreted molecules by AF-MSCs, may offer protective effects of AF-MSCs in acute liver injury. As liver injury is accompanied by a systemic inflammatory response [39], we asked if the ANXA1 effects on AHF, entail regulation of inflammatory cytokine expression. To address this question, we assessed serum levels of pro-inflammatory IFNγ and TNF and of anti-inflammatory IL-10 in AHF mice administered CM isolated from either AF-MSC-shscramble or AF-MSC-shANXA1 cultures. In line with previous reports [40] and our previous publication [15], CCl_4-induced AHF was associated with elevated circulating levels of IFNγ, TNF and IL-10 (Fig. 5c). Administration of CM from AF-MSC-shscramble but not AF-MSC-shANXA1 cultures significantly reduced IFNγ and TNF and increased IL-10 expression levels ($p < 0.05$, $p < 0.01$, $p < 0.001$, Student's *t*-test) (Fig. 5c). These data indicated a potential anti-inflammatory role of ANXA1, a molecule that has been shown to be implicated together with IFNγ and TNF, in the glucocorticoid receptor (GR) signaling canonical pathway [41] (Supplementary Fig. S2).

3.5. Secreted ANXA1 induces the proliferation of oval cells derived from AHF mice

Several reports have shown that during liver injury, oval cells reenter cell cycle, act as progenitor cells and proliferate to support liver regeneration. We have thus investigated the effect of CM from parental, shscramble and shANXA1 cultures on the proliferation of oval cells ($CD24^+/Ter119^-$) derived from AHF mice. CM from parental and shscramble cultures increased, whereas CM from shANXA1 AF-MSCs decreased oval cell proliferation, supporting the beneficial effect of ANXA1 in liver repair (Fig. 6).

4. Discussion

Accumulating evidence underscores the role of paracrine mechanisms in the regenerative potential of MSCs [16].The stem cell secretome comprises a rich source of bioactive molecules, including cytokines, chemokines and growth factors [42,43] which convey the immunoregulatory properties of MSCs and contribute to tissue repair in different pathological conditions [43]. Recent studies have demonstrated that therapies based on MSC secretome may present considerable advantages over stem cell-based applications regarding manufacturing, storage with no toxic cryopreservation agents and the loss of potency for after long periods of culture, immunogenicity, potential infections as well as time and cost effectiveness. More importantly, this cell free therapeutic approach can be manipulated for safety and dosage as a common pharmaceutical agent [44]. Thus, MSCs protect cardiomyocytes from hypoxia/reoxygenation-induced apoptosis through a mitochondrial pathway in a paracrine manner [45] and endothelial cells derived from a rat model of myocardial infarction respond to MSC secretome by increased proliferation and migration [46]. Similarly, paracrine mechanisms are important for the protective effect of MSCs in an acute kidney injury model involving secreted molecules, such as interleukins (IL-1, IL-4, IL-6, IL-10), vascular endothelial growth factor (VEGF), basic fibroblast growth factor (b-FGF), transforming

Fig. 4. Proliferation, apoptosis, clonogenic potential and migratory capacity of AF-MSCs, after knock down of ANXA1 expression. (a) Comparative analysis of the proliferation rate of AF-MSC-shANXA1 versus AF-MSC-shscramble and AF-MSC during 7 days in culture. The values presented are the mean ± SD of three independent experiments (*, $p < 0.05$; **, $p < 0.01$, Student's *t*-test). (b) Apoptosis in AF-MSCs, AF-MSC-shscramble and AF-MSC-shANXA1 was examined by FACS analysis of Annexin V staining and 7AAD was used to assess late apoptosis/necrosis. (c) The clonogenic potential of AF-MSCs, AF-MSC-shscramble and AF-MSC-shANXA1 was determined by CFU-F assay. (i): The mean numbers ± SD of CFU-F per 100 cells in a 14-day clonogenic assay are presented. The values represent the mean ± SD of three independent experiments (*, $p < 0.05$, ***, $p < 0.001$; Student's *t*-test). (ii): Representative images of the colonies formed. (d) (i) Representative diagram of the migratory potential of AF-MSCs, AF-MSC-shscramble and AF-MSC-shANXA1 to fibronectin. The values presented are the mean ± SD of three independent experiments (**, $p < 0.01$, Student's *t*-test). (ii) Representative microscopy images of the migrated AF-MSCs, AF-MSC-shscramble and AF-MSC-shANXA1. Original magnifications, (original magnification x20. scale bar: 100 μm). (e) The differentiation potential of AF-MSCs, AF-MSC-shscramble and AF-MSC-shANXA1 into HPL cells, was determined by periodic acid Schiff staining assay. (i): Quantification analysis of PAS staining. The values represent the mean ± SD of three independent experiments (*, $p < 0.05$; ***, $p < 0.001$; Student's *t*-test). (ii): Representative images of HPL, HPL-shscramble and HPL-shANXA1, after PAS staining (original magnification x20, scale bar: 100 μm).

growth factor-α (TGF-α) and B-cell lymphoma 2 (Bcl-2) [24,47]. Moreover, human umbilical cord blood-MSCs derived secretome has been shown to confer renoprotective effects, preventing diabetes kidney disease in streptozotocin-induced diabetic rats [48].

In the context of liver diseases, the paracrine protective effects of MSCs have largely been studied with respect to immunomodulation. MSCs produce IL-10 [49], IL-1 receptor antagonist (IL-1ra) [50], Hepatocyte Growth Factor (HGF) [51], VEGF and Insulin-like growth factor-binding protein (IGFBP) [52] which dampen inflammation and promote liver recovery [53–55]. Our previous work underscored the role of key important factors for AF-MSCs hepatic regeneration, such as Serpin E1, urokinase plasminogen activator, thrombospodin 1 and 2, heparin binding epidermal growth factor, fibroblast growth factor 7 and EGF. Moreover, we demonstrated the role of IL-10 derived from AF-MSCs or HPL cells in ameliorating liver damage in a mouse model of AHF [15]. More recently, we showed that conditioned medium from MSCs does not only have anti-inflammatory properties but also inhibits hepatocellular death, resulting in increased hepatocyte proliferation [56]. However, the specific factors responsible for the protective paracrine effects of AF-MSCs and HPL cells in the liver remained elusive.

Herein, we explored proteomics [28] for the definition of AF-MSC and HPL cell derived secretome. Among the various proteins identified, we selected ANXA1 for further analysis because of its reported effects on resolution of inflammation. ANXA1 is a glucocorticoid-inducible protein with cell-intrinsic and cell-extrinsic roles in limiting inflammation in diverse disease models, including rheumatoid arthritis [57], asthma, myocardial ischemia [57] and colitis [58,59]. In these studies, ANXA1 was found to downregulate the production of pro-inflammatory mediators

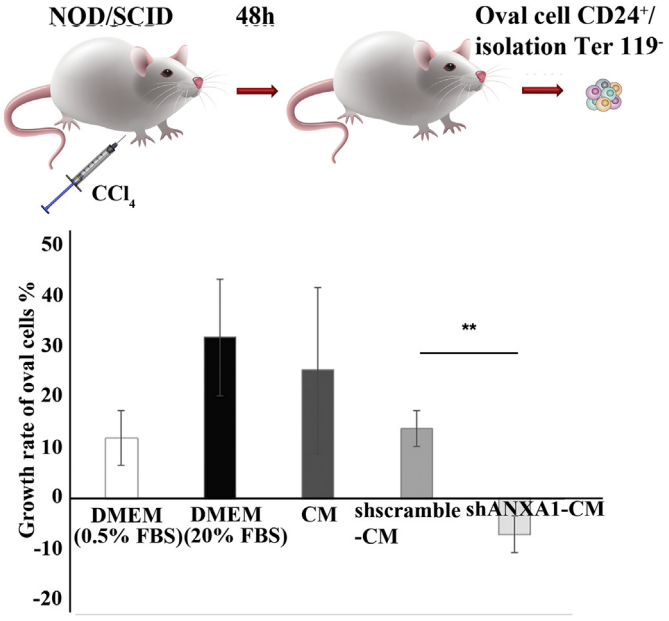

Fig. 6. Determination of the biological activity of ANXA1 on mouse oval cell proliferation after 3 days in culture. Comparative analysis of the growth rates of oval cells after treatment with DMEM supplemented with 0.5% FBS as negative control, DMEM supplemented with 20% FBS as positive control, CM from parental AF-MSCs, AF-MSC-shscramble or AF-MSC-shANXA1 cultures, during 3 days in culture. Data are presented as the mean ± SD of three independent experiments (**, $p < 0.01$; Student's *t*-test).

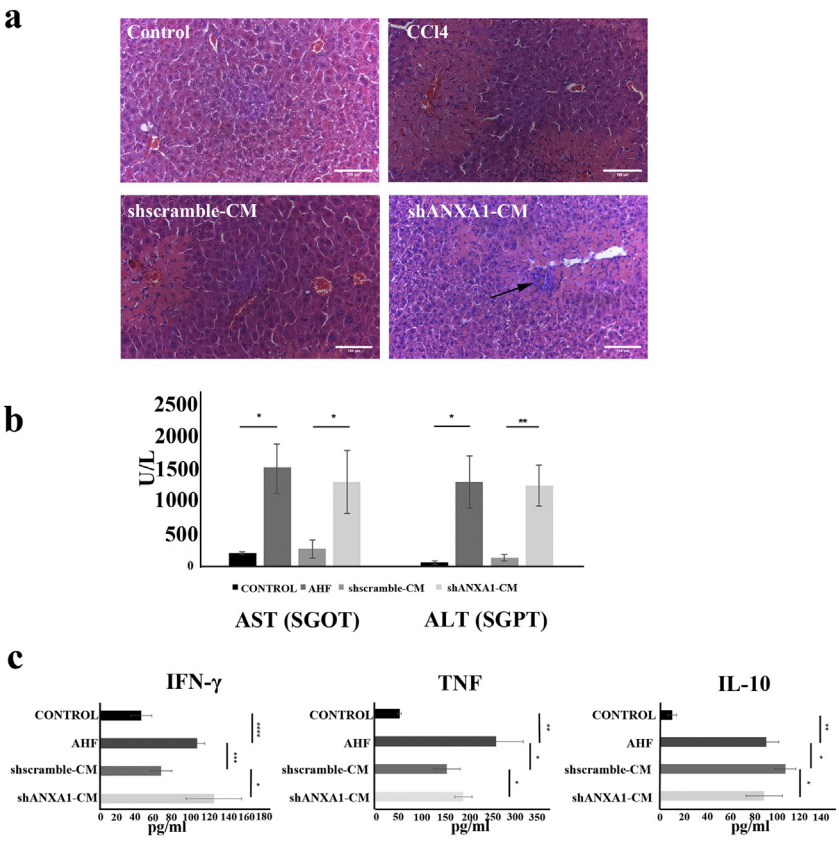

Fig. 5. Ant-inflammatory efficacy of secreted ANXA1 in AHF mouse model. (a) H&E staining of liver sections from control and AHF (CCl_4-induced) mice, as well as AHF mice receiving CM from AF-MSC-shscramble and AF-MSC-shANXA1 cultures. (Original magnification x20, scale bar: 100 μm). Arrows show necrotic areas. (b) Serum AST and ALT levels were measured in heathy mice (control), AHF mice, AHF mice that were administered CM from AF-MSC-shscramble or CM from AF-MSC-ANXA1 cultures. Data presented as the mean ± SD of five mice per group and analyzed by Student's *t*-test. P-values were estimated compared to AHF mice (*, $p < 0.05$; **, $p < 0.01$, Student's *t*-test). (c) Analysis of mouse serum cytokine levels, after treatment with shANXA1- or shscramble-CM. Mouse serum levels for IFN-γ, TNF and IL-10 from healthy mice, AHF mice or AHF mice that received shANXA1- and shscramble-CM, 24 h after administration. Each assay was performed in duplicates. Data are presented as the mean ± SD for at least 3 independent experiments and were analyzed by Student's t-test method (*, $p < 0.05$, **$p < 0.01$, ***$p < 0.001$, ****$p < 0.0001$).

including eicosanoids, nitric oxide [60], TNF and several interleukins [40,61,62]. Moreover, intracellular ANXA1 is required for the anti-inflammatory effects of glucocorticoids in vitro and in vivo [36,57,63]. The mechanism of action of ANXA1 is not fully defined. However, it has been reported that ANXA1 stimulates lipoxin A4 receptor homodimerization to increase production of IL-10 via activation of the p38 MAPK/MAPKAPK2/Hsp27 signaling cascade [64]. In turn, IL-10 suppresses the synthesis of pro-inflammatory cytokines such as IFN-γ, TNF, IL-2 and GM-CSF produced by macrophages and Th1 lymphocytes. The link between ANXA1 and IL-10 is further highlighted by the fact that Annexin-A1 failed to prevent reperfusion injury in IL-10-deficient mice [65]. Data presented herein extend the aforementioned reports by showing that ANXA1 mediates some of the anti-inflammatory properties of AF-MSC secretome by controlling systemic IL-10, IFNγ and TNF levels in AHF.

We further investigated putative links between AF-MSC-produced ANXA1 and regulation of key cellular properties of AF-MSCs. Interestingly, we found that the knock-down of ANXA1 inhibits AF-MSC proliferation and clonogenic potential in the absence of an effect on cell survival (Fig. 4). As ANXA1 has been shown to regulate cell migration and promote tissue repair [65,66], we also evaluated the migratory capacity of AF-MSCs under conditions of reduced expression of ANXA1. Our results demonstrated that inhibition of ANXA1 expression led to decreased cell migration (Fig. 4), confirming the significant role of ANXA1 in tissue regeneration. Importantly, the knock-down of ANXA1 also impaired the differentiation of AF-MSCs to hepatic progenitors (Fig. 4).

As administration of conditioned medium from AF-MSCs had a profound effect on histological and biochemical (AST/ALT) markers of liver damage, we hypothesized that ANXA1 may mediate additional therapeutic functions beyond regulation of inflammation. In line with this hypothesis, conditioned medium from AF-MSCs lacking ANXA1 reduced the proliferation of isolated mouse liver progenitors (oval cells), further supporting the important role of ANXA1 in hepatic proliferation and liver regeneration.

The findings reported herein expand our understanding of the mechanisms by which MSCs confer therapeutic effects in AHF. Our study provides the first detailed analysis of AF-MSC and hepatic progenitor-like cell-derived secretome and shows an important role of AF-MSC-produced ANXA1 in ameliorating liver damage. Importantly, we demonstrate that the effects of ANXA1 on disease severity exceed its established role in the resolution of inflammation to include effects on progenitor cell proliferation, migration and differentiation. Collectively, these data may have important ramifications for the development of cell free, non-invasive, less immunogenic and non-toxic strategies for the management of AHF.

Supplementary data to this article can be found online at https://doi.org/10.1016/j.ebiom.2019.07.009.

Acknowledgements

We would like to thank Professor Despina Perrea and Mr. Nikos Tsakiropoulos for biochemical analyses of mouse blood sera, Prof M. Gazouli and Dr. Evangelia Kourepini for their valuable assistance in ELISA experiments, Mr. Konstantinos Paschidis for his assistance in animal work and Dr. E. Rigana and Dr. S. N. Pagakis for their assistance in biological imaging.

Grant acknowledgment

This research has been funded by the Fondation Santé research grant (No 70/3/13455) and GILEAD Asklipeios Grant (No 73/15036) to MR and Postdoctoral Fellowships of Excellence – Siemens IKY Foundation to OT. Moreover, this research is co-financed by Greece and the European Union (European Social Fund- ESF) through the Operational Programme «Human Resources Development, Education and Lifelong Learning» in the context of the project "Reinforcement of Postdoctoral Researchers" (MIS-5001552), implemented by the State Scholarships Foundation (IKϒ) to DZ. The funders had no role in study design, data collection, data analysis, interpretation and writing of the report.

Disclosure of potential conflicts of interest

The authors indicate no potential conflicts of interest.

Authorship contribution

Dimitra Zagoura: Experimental design, in vivo and in ex vivo experiments, data analysis and interpretation, manuscript writing and final approval of manuscript.

Ourania Trohatou: Experimental design, in vitro experimental procedures, data analysis and interpretation, manuscript writing and final approval of manuscript.

Manousos Makridakis: proteomics data, data analysis and interpretation, manuscript writing and final approval of manuscript.

Antonia Kollia: Experimental design proteomics data and data analysis and interpretation and final approval of manuscript.

Nikolitsa Kokla: in vitro experimental procedures, data analysis and interpretation.

Marika Mokou: Protein analysis and data analysis and interpretation and final approval of manuscript.

Adriana Psaraki: ex vivo experiments, data analysis and final approval of manuscript.

Aristides G Eliopoulos: Data analysis, manuscript writing and final approval of manuscript.

Antonia Vlahou: proteomics data, data analysis and interpretation, manuscript writing and final approval of manuscript.

Maria G Roubelakis: Conception and design, financial support, experimental procedures, data analysis and interpretation, manuscript writing and final approval of manuscript.

References

[1] Prockop DJ. Marrow stromal cells as stem cells for continual renewal of nonhematopoietic tissues and as potential vectors for gene therapy. J Cell Biochem 1998(30−31):284–5.
[2] Linero I, Chaparro O. Paracrine effect of mesenchymal stem cells derived from human adipose tissue in bone regeneration. PLoS One 2014;9(9):e107001.
[3] Andrzejewska A, Lukomska B, Janowski M. Concise review: Mesenchymal stem cells: from roots to boost. Stem Cells 2019;37:855–64.
[4] Galipeau J, Sensebe L. Mesenchymal stromal cells: clinical challenges and therapeutic opportunities. Cell Stem Cell 2018;22(6):824–33.
[5] Baraniak PR, McDevitt TC. Stem cell paracrine actions and tissue regeneration. Regen Med 2010;5(1):121–43.
[6] Fu Y, Karbaat L, Wu L, Leijten J, Both SK, Karperien M. Trophic effects of mesenchymal stem cells in tissue regeneration. Tissue Eng Part B Rev 2017;23(6):515–28.
[7] Wang M, Yuan Q, Xie L. Mesenchymal stem cell-based immunomodulation: properties and clinical application. Stem Cells Int 2018;2018:3057624.
[8] Dimarino AM, Caplan AI, Bonfield TL. Mesenchymal stem cells in tissue repair. Front Immunol 2013;4:201.
[9] Squillaro T, Peluso G, Galderisi U. Clinical trials with mesenchymal stem cells: an update. Cell Transplant 2016;25(5):829–48.
[10] Wang LT, Ting CH, Yen ML, et al. Human mesenchymal stem cells (mscs) for treatment towards immune- and inflammation-mediated diseases: review of current clinical trials. J Biomed Sci 2016;23(1):76.
[11] Choi JR, Yong KW, Nam HY. Current status and perspectives of human mesenchymal stem cell therapy. Stem Cells Int 2019;4762634.
[12] Davies JE, Walker JT, Keating A. Concise review: Wharton's jelly: the rich, but enigmatic, source of mesenchymal stromal cells. Stem Cells Transl Med 2017;6(7):1620–30.
[13] Konala VB, Mamidi MK, Bhonde R, Das AK, Pochampally R, Pal R. The current landscape of the mesenchymal stromal cell secretome: a new paradigm for cell-free regeneration. Cytotherapy 2016;18(1):13–24.
[14] Kay AG, Long G, Tyler G, et al. Mesenchymal stem cell-conditioned medium reduces disease severity and immune responses in inflammatory arthritis. Sci Rep 2017;7(1):18019.
[15] Zagoura DS, Roubelakis MG, Bitsika V, et al. Therapeutic potential of a distinct population of human amniotic fluid mesenchymal stem cells and their secreted molecules in mice with acute hepatic failure. Gut 2012;61(6):894–906.
[16] Rani S, Ryan AE, Griffin MD, Ritter T. Mesenchymal stem cell-derived extracellular vesicles: toward cell-free therapeutic applications. Mol Ther 2015;23(5):812–23.

[17] Kim HK, Lee SG, Lee SW, et al. A subset of paracrine factors as efficient biomarkers for predicting vascular regenerative efficacy of mesenchymal stromal/stem cells. Stem Cells 2018;37(1):77–88.
[18] Roubelakis MG, Bitsika V, Zagoura D, et al. In vitro and in vivo properties of distinct populations of amniotic fluid mesenchymal progenitor cells. J Cell Mol Med 2011;15(9):1896–913.
[19] Roubelakis MG, Pappa KI, Bitsika V, et al. Molecular and proteomic characterization of human mesenchymal stem cells derived from amniotic fluid: comparison to bone marrow mesenchymal stem cells. Stem Cells Dev 2007;16(6):931–52.
[20] Trohatou O, Anagnou NP, Roubelakis MG. Human amniotic fluid stem cells as an attractive tool for clinical applications. Curr Stem Cell Res Ther 2013;8(2):125–32.
[21] Trohatou O, Roubelakis MG. Mesenchymal stem/stromal cells in regenerative medicine: past, present, and future. Cell Reprogram 2017;19(4):217–24.
[22] Zagoura DS, Trohatou O, Bitsika V, et al. Af-mscs fate can be regulated by culture conditions. Cell Death Dis 2013;4:e571.
[23] in 't Aker PS, Noort WA, Scherjon SA, et al. Mesenchymal stem cells in human second-trimester bone marrow, liver, lung, and spleen exhibit a similar immunophenotype but a heterogeneous multilineage differentiation potential. Haematologica 2003;88(8):845–52.
[24] Tsai MS, Hwang SM, Tsai YL, Cheng FC, Lee JL, Chang YJ. Clonal amniotic fluid-derived stem cells express characteristics of both mesenchymal and neural stem cells. Biol Reprod 2006;74(3):545–51.
[25] Olivo R, Guarrera JV, Pyrsopoulos NT. Liver transplantation for acute liver failure. Clin Liver Dis 2016;22(2):409–17.
[26] Cainelli F, Nardo B, Viderman D, Dzudzor B, Tachi K, Vento S. Treatment of acute liver failure in resource-constrained settings without transplantation facilities can be improved. Front Med (Lausanne) 2016;3:31.
[27] Wang DW, Yin YM, Yao YM. Advances in the management of acute liver failure. World J Gastroenterol 2013;19(41):7069–77.
[28] Makridakis M, Roubelakis MG, Bitsika V, et al. Analysis of secreted proteins for the study of bladder cancer cell aggressiveness. J Proteome Res 2010;9(6):3243–59.
[29] Makridakis M, Vlahou A. Gelc-ms: a sample preparation method for proteomics analysis of minimal amount of tissue. Methods Mol Biol 2018;1788:165–75.
[30] Trohatou O, Zagoura D, Orfanos NK, et al. Mir-26a mediates adipogenesis of amniotic fluid mesenchymal stem/stromal cells via pten, cyclin e1, and cdk6. Stem Cells Dev 2017;26(7):482–94.
[31] Trohatou O, Zagoura D, Bitsika V, et al. Sox2 suppression by mir-21 governs human mesenchymal stem cell properties. Stem Cells Transl Med 2014;3(1):54–68.
[32] Roubelakis MG, Trohatou O, Roubelakis A, et al. Platelet-rich plasma (prp) promotes fetal mesenchymal stem/stromal cell migration and wound healing process. Stem Cell Rev 2014;10(3):417–28.
[33] Filip S, Vougas K, Zoidakis J, et al. Comparison of depletion strategies for the enrichment of low-abundance proteins in urine. PLoS One 2015;10(7):e0133773.
[34] Papaleo E, Gromova I, Gromov P. Gaining insights into cancer biology through exploration of the cancer secretome using proteomic and bioinformatic tools. Expert Rev Proteomics 2017;14(11):1021–35.
[35] Masson NM, Currie IS, Terrace JD, Garden OJ, Parks RW, Ross JA. Hepatic progenitor cells in human fetal liver express the oval cell marker thy-1. Am J Physiol Gastrointest Liver Physiol 2006;291(1):G45–54.
[36] Hannon R, Croxtall JD, Getting SJ, et al. Aberrant inflammation and resistance to glucocorticoids in annexin 1−/− mouse. FASEB J 2003;17(2):253–5.
[37] Neymeyer H, Labes R, Reverte V, et al. Activation of annexin a1 signalling in renal fibroblasts exerts antifibrotic effects. Acta Physiol (Oxf) 2015;215(3):144–58.
[38] Perretti M, Di Filippo C, D'Amico M, Dalli J. Characterizing the anti-inflammatory and tissue protective actions of a novel annexin a1 peptide. PLoS One 2017;12(4):e0175786.
[39] Vyrla D, Nikolaidis G, Oakley F, et al. Tpl2 kinase is a crucial signaling factor and mediator of nkt effector cytokine expression in immune-mediated liver injury. J Immunol 2016;196(10):4298–310.
[40] Sugimoto MA, Vago JP, Teixeira MM, Sousa LP. Annexin a1 and the resolution of inflammation: modulation of neutrophil recruitment, apoptosis, and clearance. J Immunol Res 2016;8239258.
[41] Van Bogaert T, De Bosscher K, Libert C. Crosstalk between tnf and glucocorticoid receptor signaling pathways. Cytokine Growth Factor Rev 2010;21(4):275–86.
[42] Skalnikova H, Motlik J, Gadher SJ, Kovarova H. Mapping of the secretome of primary isolates of mammalian cells, stem cells and derived cell lines. Proteomics 2011;11(4):691–708.
[43] Makridakis M, Roubelakis MG, Vlahou A. Stem cells: insights into the secretome. Biochim Biophys Acta 2013;1834(11):2380–4.
[44] Vizoso FJ, Eiro N, Cid S, Schneider J, Perez-Fernandez R. Mesenchymal stem cell secretome: toward cell-free therapeutic strategies in regenerative medicine. Int J Mol Sci 2017;18(9).
[45] Xiang MX, He AN, Wang JA, Gui C. Protective paracrine effect of mesenchymal stem cells on cardiomyocytes. J Zhejiang Univ Sci B 2009;10(8):619–24.
[46] Bollini S, Gentili C, Tasso R, Cancedda R. The regenerative role of the fetal and adult stem cell secretome. J Clin Med 2013;2(4):302–27.
[47] Glorieux G, Mullen W, Duranton F, et al. New insights in molecular mechanisms involved in chronic kidney disease using high-resolution plasma proteome analysis. Nephrol Dial Transplant 2015;30(11):1842–52.
[48] Park JH, Hwang I, Hwang SH, Han H, Ha H. Human umbilical cord blood-derived mesenchymal stem cells prevent diabetic renal injury through paracrine action. Diabetes Res Clin Pract 2012;98(3):465–73.
[49] Aggarwal S, Pittenger MF. Human mesenchymal stem cells modulate allogeneic immune cell responses. Blood 2005;105(4):1815–22.
[50] Rasmusson I, Ringden O, Sundberg B, Le Blanc K. Mesenchymal stem cells inhibit lymphocyte proliferation by mitogens and alloantigens by different mechanisms. Exp Cell Res 2005;305(1):33–41.
[51] Di Nicola M, Carlo-Stella C, Magni M, et al. Human bone marrow stromal cells suppress t-lymphocyte proliferation induced by cellular or nonspecific mitogenic stimuli. Blood 2002;99(10):3838–43.
[52] Parekkadan B, van Poll D, Suganuma K, et al. Mesenchymal stem cell-derived molecules reverse fulminant hepatic failure. PLoS One 2007;2(9):e941.
[53] Abdel Aziz MT, Atta HM, Mahfouz S, et al. Therapeutic potential of bone marrow-derived mesenchymal stem cells on experimental liver fibrosis. Clin Biochem 2007;40(12):893–9.
[54] Fang B, Shi M, Liao L, Yang S, Liu Y, Zhao RC. Systemic infusion of flk1(+) mesenchymal stem cells ameliorate carbon tetrachloride-induced liver fibrosis in mice. Transplantation 2004;78(1):83–8.
[55] Zhao DC, Lei JX, Chen R, et al. Bone marrow-derived mesenchymal stem cells protect against experimental liver fibrosis in rats. World J Gastroenterol 2005;11(22):3431–40.
[56] Xagorari A, Siotou E, Yiangou M, et al. Protective effect of mesenchymal stem cell-conditioned medium on hepatic cell apoptosis after acute liver injury. Int J Clin Exp Pathol 2013;6(5):831–40.
[57] Patel HB, Kornerup KN, Sampaio AL, et al. The impact of endogenous annexin a1 on glucocorticoid control of inflammatory arthritis. Ann Rheum Dis 2012;71(11):1872–80.
[58] Babbin BA, Laukoetter MG, Nava P, et al. Annexin a1 regulates intestinal mucosal injury, inflammation, and repair. J Immunol 2008;181(7):5035–44.
[59] Cobos Caceres C, Bansal PS, Navarro S, et al. An engineered cyclic peptide alleviates symptoms of inflammation in a murine model of inflammatory bowel disease. J Biol Chem 2017;292(24):10288–94.
[60] Ferlazzo V, D'Agostino P, Milano S, et al. Anti-inflammatory effects of annexin-1: stimulation of il-10 release and inhibition of nitric oxide synthesis. Int Immunopharmacol 2003;3(10−11):1363–9.
[61] Feng J, Wang X, Li H, Wang L, Tang Z. Silencing of annexin a1 suppressed the apoptosis and inflammatory response of preeclampsia rat trophoblasts. Int J Mol Med 2018;42(6):3125–34.
[62] Guido BC, Zanatelli M, Tavares-de-Lima W, Oliani SM, Damazo AS. Annexin-a1 peptide down-regulates the leukocyte recruitment and up-regulates interleukin-10 release into lung after intestinal ischemia-reperfusion in mice. J Inflamm (Lond) 2013;10(1):10.
[63] Yang YH, Aeberli D, Dacumos A, Xue JR, Morand EF. Annexin-1 regulates macrophage il-6 and tnf via glucocorticoid-induced leucine zipper. J Immunol 2009;183(2):1435–45.
[64] Filep JG. Biasing the lipoxin a4/formyl peptide receptor 2 pushes inflammatory resolution. Proc Natl Acad Sci U S A 2013;110(45):18033–4.
[65] Souza DG, Fagundes CT, Amaral FA, et al. The required role of endogenously produced lipoxin a4 and annexin-1 for the production of il-10 and inflammatory hyporesponsiveness in mice. J Immunol 2007;179(12):8533–43.
[66] Ernst S, Lange C, Wilbers A, Goebeler V, Gerke V, Rescher U. An annexin 1 n-terminal peptide activates leukocytes by triggering different members of the formyl peptide receptor family. J Immunol 2004;172(12):7669–76.